

Analysis of a novel human gene, LOC92912, over-expressed in hypopharyngeal tumours

Atefeh Seghatoleslam^a, Alberto Zambrano^a, Regine Millon^b, Gitali Ganguli^a,
Manuela Argentini^a, Anne Cromer^a, Joseph Abecassis^b, Bohdan Wasylyk^{a,*}

^a *Institut de Génétique et de Biologie Moléculaire et Cellulaire (IGBMC), CNRS/INSERM/ULP, 1 Rue Laurent Fries, BP 10142, Illkirch Cedex, Strasbourg 67404, France*

^b *UPRES EA 34-30, Centre de Lutte Contre le Cancer Paul Strauss, 3 rue de la porte de l'hôpital. BP 42, 67065 Strasbourg Cedex, France*

Received 31 October 2005

Available online 14 November 2005

Abstract

We have identified by differential display a number of novel genes that are expressed in hypopharyngeal head and neck squamous cell carcinoma. We report here the characterisation of one of these novel human genes, **LOC92912**, that encodes a protein of 375 amino acids. The protein contains a RWD domain, a coiled-coil, and an E2 ubiquitin conjugating enzyme domain. **LOC92912** is upregulated in about 85% of tumour samples. It is expressed in tumour masses and in invasive epithelium, and is located in the cytoplasm of cells. To gain insights into its functions, we identified potential interacting partners by immunoaffinity purification of the flag tagged protein followed by MALDI peptide mass fingerprinting mass spectrometry. Actin and six actin-binding proteins were unambiguously identified as potential interacting partners, suggesting that **LOC92912**'s functions may be linked with the cytoskeleton. This novel human gene may represent a new target for cancer therapeutics.

© 2005 Elsevier Inc. All rights reserved.

Keywords: RWD domain; E2 ubiquitin conjugating enzyme; HNSCC; Cytoskeleton; Actin

Head and neck squamous cell carcinoma (HNSCC) arises from the surface epithelium of the upper-aerodigestive tract (hypopharynx, pharynx, larynx, and oral cavity). The annual incidence is 500,000 cases [1], and in the vast majority of patients it is associated with a history of alcohol and tobacco consumption [2,3]. However, the pathogenesis of the disease may also be associated with genetic and other risk factors [4]. Treatment of HNSCC is currently based on single or multimodality therapy, including surgical resection, radiation, and/or chemotherapy. Unfortunately these strategies have had little impact on survival over last 20 years [5]. There is a dearth of biomarkers, and they have not been included in clinical work-up strategies for patients nor used in prospective trials to randomise patients for

different treatment modalities [6]. In general, HNSCC proliferates rapidly, is locally aggressive, and metastasises to cervical lymph nodes [2]. Many of the critical biological processes in HNSCC are, as of yet, unidentified. One approach to uncover these pathways is to study novel genes with altered expression, in order to isolate elements involved in the genesis, progression, and metastasis of tumours. We have performed genomewide screens of the HNSCC transcriptome using differential display (DD) and DNA microarrays ([7,8] and ongoing studies). These efforts have pinpointed a number of genes that are upregulated in the cancer compared with the corresponding normal tissue from the same patients. Since carcinogenesis involves activation of oncogenes and/or inactivation of tumour suppressor genes, enhanced expression of at least some of these upregulated genes may reflect their oncogenic properties.

In the present study, we report an analysis of one of the novel sequences we identified by differential display. We

* Corresponding author. Fax: +33 3 88 65 32 02.

E-mail address: boh@igbmc.u-strasbg.fr (B. Wasylyk).

found that it corresponds to the EST **LOC92912**, and the UniGene cluster **HS.23033** (<http://www.ncbi.nlm.nih.gov/UniGene/>). We showed that it is upregulated in cancer tissues compared to the corresponding noncancerous uvula epithelium. It localises mostly to the cytoplasm of epithelial cells and is expressed in several HNSCC cell lines as a polypeptide of 43 kDa. When the flagged protein was purified by immunoaffinity and subjected to mass spectrometry analysis, several additional proteins were identified, including actin and actin-associated proteins, suggesting that the function of **LOC92912** may be associated with the cytoskeleton.

Materials and methods

Tissue samples. HNSCC tumour samples and the corresponding histologically normal tissues were derived from surgical resections of HNSCC (informed consent was given in all cases). The patients had not been treated at the time of surgery, but were subsequently treated with radiotherapy. The samples were from the advancing edges of the tumours excluding the necrotic centres and were comprised of 70–80% cancer cells in almost all cases. Normal samples were collected from the farthest margin of the surgical resections (usually uvula).

Quantitative real time PCR (QRT-PCR). Reverse transcription was performed with 1 µg total RNA, random primers, and the Superscript II RT-PCR system (Life Technologies). PCRs were done using the Light Cycler (Roche Diagnostics, Meylan, France) with the LC Fast start DNA master SYBR green I reaction mixture according to the manufacturer's instructions. 2 microlitres of 1:100 diluted reverse transcriptase products was used in 20 µl reaction volumes. The primers were chosen with Primer3 software (http://frodo.wi.mit.edu/cgi-bin/primer3/primer3_www.cgi) in order to amplify exon–exon junction containing regions. The specificity of the primers was verified by Blast analysis at NCBI and by agarose gel analysis of the PCR products. The primer sequences were: 5'-CCGTGGGTAGTGGTTGATCT-3' and 5'-AGCGATTCCGCATCGT CAGT-3' for **LOC92912** gene and 5'-GAAGGCTGTGGTGCTGATGG-3' and 5'-CCGGATATGAGGCAGCAGTT-3' for the ubiquitous internal control gene, ribosomal phospho-protein P0 (RPLP0). For each gene, a standard curve was constructed using serial dilutions of standard cDNAs (equivalent to 100, 40, 20, 10, 4, 2, and 1 ng total RNA) derived from a pool of 10 hypopharyngeal tumours. The concentrations of primers, MgCl₂, probes, and cDNA were optimised to obtain linear standard curves. Unknown samples were estimated relative to these standard curves. PCRs were run at least twice for each sample. The mean value was retained whenever the standard deviation did not exceed 15%. The median of the N samples was given an arbitrary unit of 1. All values were normalised using RPLP0 as an internal control. RPLP0 (originally called 36B4) is a ubiquitously expressed gene that has been routinely used in different laboratories as an internal control to normalise for the amount of RNA. In a large study (98 cases), we confirmed by QRT-PCR that its expression level remains relatively constant between HNSCC tumours and matched normal tissues (data not shown). RPLP0 gave better results than the commonly used control GAPDH, which was more variable between samples in our experiments. Student's *t* test was used for statistical analysis between tumour and normal sample populations.

Generation of **LOC92912 antibodies.** Three different peptides, p-1: LDELHCQFLVPQGGSPHSL, p-2: EDTKNNLLRQQLKWLIC, and p-3: LPTGQNGTTEVTSEE corresponding to **LOC92912** amino acid sequence 31–49, 87–104, and 125–140, respectively, were designed using GCG10 and Sequence Retrieval Software (<http://igbmc.u-strasbg.fr/EM-BOSS/>). Peptide specificity was checked by BlastP at NCBI. A cysteine residue was added to one end of the peptide where necessary. The peptides were coupled to ovalbumin (Imject Maleimide, Pierce) and used to immunise six rabbits (two rabbits for each peptide). Individual sera were screened using Western blot analysis of endogenous and flagged-

LOC92912 transfected cell lysates (data not shown). Sera from rabbits immunised with p-3 gave the best results with endogenous and transfected **LOC92912**, and were used for the present study.

Immunohistochemistry. Immunohistochemistry (IHC) was performed on 5-µm thick formalin-fixed paraffin-embedded tissue sections using polyclonal antibodies raised against **LOC92912** according to a standard horseradish peroxidase (HRP) protocol. Tissue sections were deparaffinised in xylene, rehydrated in decreasing ethanol concentrations, heated in citrate buffer, pH 6, in a microwave oven for 30 min (to retrieve antigens), washed, treated for 10 min with 3% H₂O₂ in methanol (to inactivate endogenous peroxidase activity), blocked for 1 h in Tris-buffered saline solution containing 5% skimmed-milk powder and 0.5% Tween 20 (TBSTM5), and incubated overnight with antibody diluted 1:500 or 1:1000 in TBSTM2 at 4 °C. They were stained with a broad spectrum HRP-DAB Kit according to the manufacturer's protocol (Zymed PicTure PLUS Kit, Broad Spectrum, DAB, Zymed), washed, and counterstained with Gill's hematoxylin solution (Sigma) or methyl green (DAKO). Specificity of staining was verified by including a control antibody (DAKO Cytomation) or pre-immune serum, or by omitting the primary antibody.

In situ hybridisation (ISH). For ISH, 5-µm thick sections were deparaffinised, rehydrated in decreasing concentrations of ethanol, air-dried, washed in PBS three times for 10 min each, permeabilised by proteolytic digestion with proteinase K (6 µg/ml in 50 mM Tris–HCl, pH 7.6) at 50 °C for 10 min, rinsed twice in PBS for 5 min each, and heated at 92 °C for 2 min in a heat block. The slides were placed in PBS for 5 min, 0.2 N HCl for 20 min, and PBS for 5 min, dehydrated through washes in graded ethanol for 5 min each, placed in 2× SSC at 70 °C for 5 min, 92 °C for 5 min, and immediately covered with heat denatured digoxigenin-labelled probes diluted 1/50 in hybridisation buffer (50% deionised formamide, 10% dextran sulphate, 1 mg/ml tRNA, 1× Denhardt's solution, and 1× salt buffer). The slides were incubated at 65 °C overnight in a humidity chamber, washed four times for 15 min with pre-warmed washing solution (1× SSC, 50% formamide, and 0.1% Tween 20) at 65 °C, two times 30 min each with MABT buffer (100 mM maleic acid, 150 mM NaCl, and 0.1% Tween 20) at room temperature, and covered with freshly prepared antibody blocking solution [60% (v/v) MABT, 20% (v/v) goat immunoglobulin, and 2% blocking reagent (Roche)] 1 h at room temperature. The sections were covered with goat anti-digoxigenin antibodies coupled to alkaline-phosphatase (Roche) (1/2000 in antibody blocking solution) and incubated 4 h at 37 °C in a humidity chamber. The slides were washed two times 30 min each in MABT buffer and rinsed two times for 10 min at room temperature with NTMT buffer (100 mM Tris–HCl, pH 9.5, 100 mM NaCl, 50 mM MgCl₂, and 0.1% Tween 20). The slides were covered with alkaline-phosphatase substrate solution (NBT, BCIP) containing levamisole and incubated for a few hours at room temperature or overnight at 4 °C in a humidity chamber. The reaction was stopped by washing with 0.1% Tween 20 in PBS, and the tissues were counterstained with nuclear fast red (Vector Labs) and mounted. Specific sense and antisense probes were synthesised by in vitro transcription of the **LOC92912** expression vector in the presence of digoxigenin-labelled UTP.

Cell culture, expression vectors, and transfections. HEP-2, HaCaT, RPMI 2650 cells, and other HNSCC cell lines were maintained as recommended by ATCC (American Type Cell Collection). Transfections were performed by the calcium–phosphate method on RPMI 2650 cells. To obtain stable clones, transfected cells were trypsinised 48 h post-transfection and passaged into medium containing puromycin (2 µg/ml). The selection medium was replaced every 3 days and clones were isolated 20–24 days post-transfection. Typically, seven clones were isolated per stable transfection and shown to express **LOC92912** by Western blotting. **LOC92912** cDNA clone was obtained from ATCC (ATCC catalogue No. 6394363; IMAGE clone ID: 3907760; GenBank ID BC017708; human uterus). The coding region was PCR-amplified using oligonucleotides containing *Bam*HI restriction sites (CGCGGATCCCATTTAGCCATCTTCCTTTGGAGG and CGCGGATCCCATGTCCGTGTCAGGGCTCAAG) and cloned into the pSG5-puro-flag expression vector (IGBMC facility) to obtain sense and antisense versions of the recombinants.

Western blotting. Cells growing in culture plates were rinsed twice in ice-cold PBS, scraped, and centrifuged. The cell pellet was lysed in

extraction buffer [50 mM Tris-HCl, pH 8, 5 mM EDTA, pH 8, 150 mM NaCl, 1% Nonidet-P 40, 0.02% sodium azide, 1 mM PMSF, and 1× PIC (protease inhibitor cocktail, Amersham)]. Lysates were sonicated at 0 °C for 30 s and then cleared by centrifugation. Protein concentrations were measured by the Bradford method and 40 µg of total protein was fractionated on 8% SDS-PAGE and transferred to nitrocellulose membranes. The membranes were blocked for 1 h in 5% dried-fat free milk, 0.05%

Tween 20 in PBS and incubated 2 h with specific antibodies diluted in blocking solution. Antibodies used: polyclonal serum against LOC92912 (1/500), TATA box binding protein (TBP) (1/2000; IGBMC monoclonal antibody facility), and anti-flag (1/2000; IGBMC monoclonal antibody facility). Blots were washed and incubated with specific secondary antibodies coupled to HRP (Jackson ImmunoResearch) and revealed with enhanced chemiluminescence reagents (ECL, Pierce).

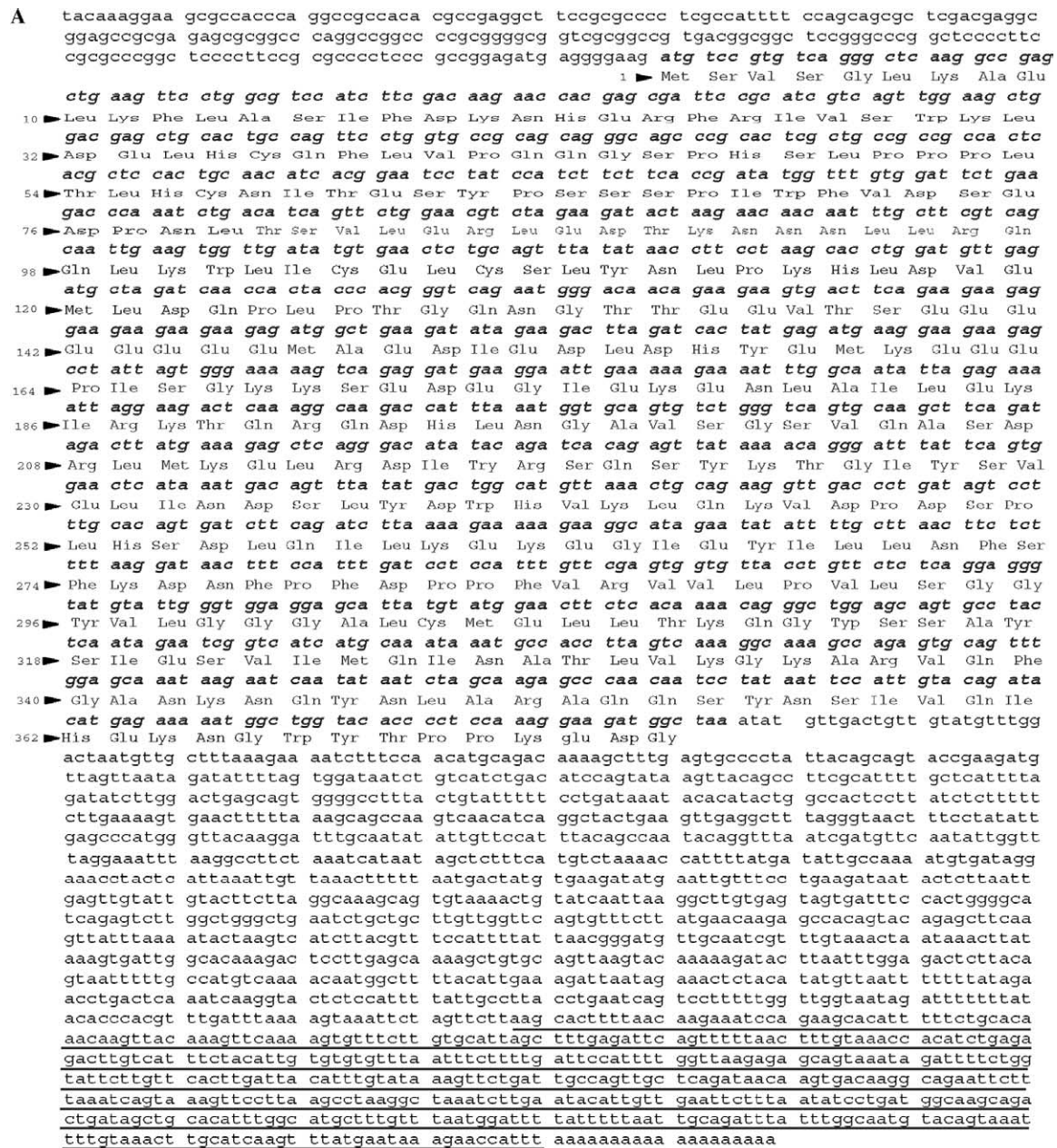


Fig. 1. Coding sequence and predicted protein expressed by the LOC92912 gene. (A) The complete coding sequence (Accession No. BC017708 in GenBank database, nt.1–2939) and the corresponding amino acid sequence (1–375) of *Homo sapiens* hypothetical protein LOC92912 is shown. Underlined and bold letters represent the sequence derived from differential display and the coding sequence of LOC92912, respectively. (B) The predicted LOC92912 domain architecture includes an RWD domain (amino acids 8–123), a coiled-coil sequence (amino acids 133–163), and a ubiquitination conjugating domain UQ-CON (amino acids 207–368).

Immunofluorescence. Cells grown on coverslips were fixed in methanol (-20°C) for 5 min, acetone (-20°C) for 30 s, permeabilised for 5 min with 0.1% Triton X-100 in PBS, blocked with 1% BSA in PBS, and then incubated with polyclonal antibodies raised against **LOC92912** antibodies (diluted 1/500 with 1% BSA in PBS), followed by secondary antibodies coupled to Cy3 (Jackson ImmunoResearch). Slides were mounted with Vectashield (Vector) containing DAPI, images were acquired with a Lecia DMLB and analysed with CoolSnap software.

Purification of flagged-protein and MALDI mass spectrometry. Flagged-proteins were purified from stable transfectants by immunoaffinity with anti-flag M2 resin (Sigma) following the manufacturer's instructions. As negative controls, we always performed, in parallel, affinity purification on cell extracts from empty and antisense stable transfectants. We have also purified other flagged-proteins and found different co-eluting proteins. Proteins were eluted by competition with flag peptide, dialysed, concentrated with Centricon columns (Millipore), and fractionated by 8% SDS-PAGE. The gels were stained with Coomassie or silver salts. Excised bands were digested as previously described [9] with 5–10 μl (depending on the gel volume) of 10 ng/ μl of freshly diluted trypsin in 25 mM NH_4HCO_3 overnight at 30°C . Five microlitres of 40% $\text{H}_2\text{O}/60\%$ acetonitrile/0.1% TFA was added and after 4 h at room temperature, the mixture was sonicated for 2 min and centrifuged. 0.5 μl of the supernatant was mixed with an equal volume of saturated DHB (Sigma) dissolved in 20% acetonitrile and applied to the target. MALDI mass measurements were carried out on a Bruker Reflex IV MALDI-TOF spectrometer, using a maximum accelerating potential of 20 kV in the positive reflector mode. The acquisition mass range was 800–3000 Da with the low mass gate set at 700 Da. Internal calibration was performed using autolytic trypsin peptides (MH^+ : $m/z = 842.51$ and $m/z = 2211.11$). Monoisotopic peptide

masses were assigned using the Bruker Flex Analysis software. The ProFound program was used for database searching (<http://prowl.rockefeller.edu/>) with the following parameters: database NCBI, taxonomy mammalia, protein mass range 0–150 kDa, trypsin digestion with one missed cleavage allowed, cysteines modified by carbamidomethylation, methionine oxidation, and mass tolerance of 75 ppm.

Results

Isolation and bioinformatic analysis of **LOC92912**

We identified by differential display a 445 base-pair (bp) fragment that was over-expressed in hypopharyngeal HNSCC compared to normal tissues (Fig. 1). We found, by BLAST analysis against the human genome database (NCBI), that it corresponded precisely to the 3' terminus of a novel human gene, **LOC92912**, that is located on chromosome 15 (15q23) and has 13 exons distributed over 57.6 kb [location: 73,922,855–73,980,435 (NT_010194), Ensembl Human Exon View]. The cDNA is 2939 bp long and has an open reading frame (ORF) of 1339 bp that codes for a protein of 375 amino acids (molecular weight 42.818 kDa, isoelectric point 4.6, and charge -18.0). There are related proteins in organisms as diverse as humans and worms [percentage identity and length of aligned region:

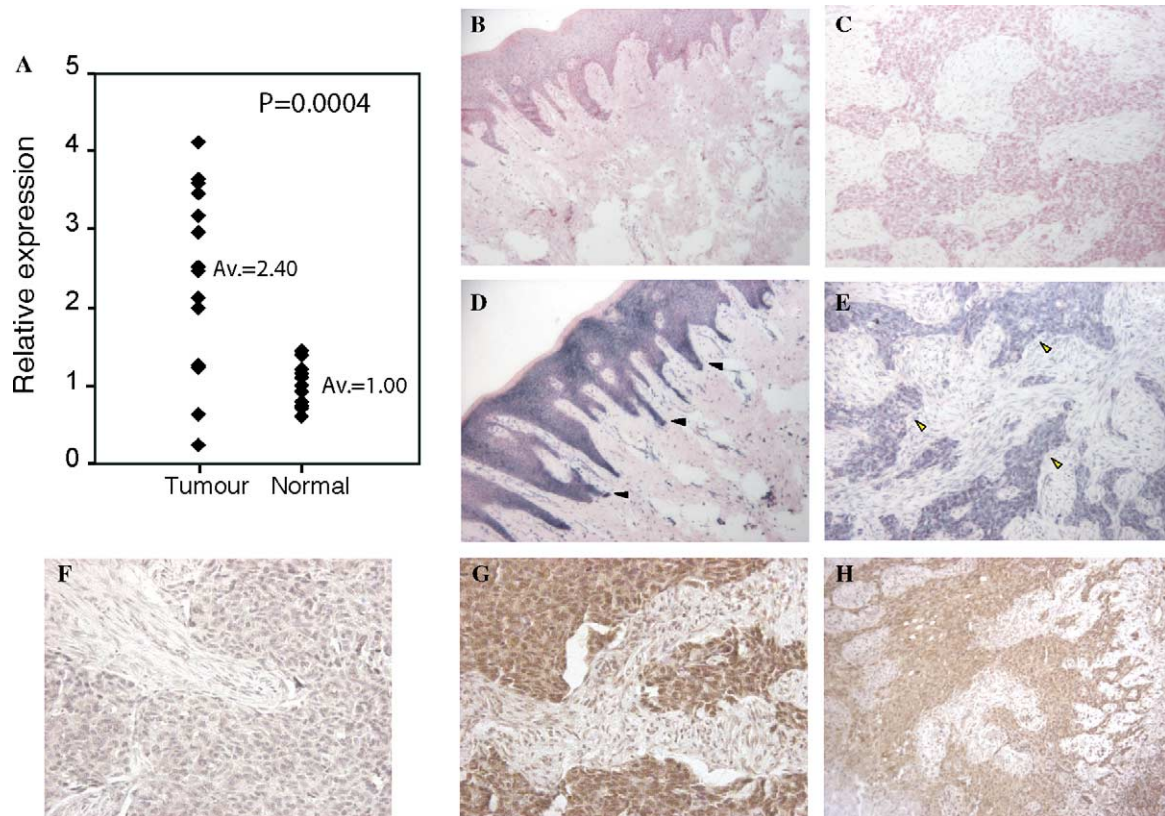


Fig. 2. **LOC92912** is over-expressed in HNSCC. (A) QRT-PCR using specific primers for **LOC92912** (see Materials and methods). The average (Av.) over-expression is 2.4-fold in tumour compared to matched normal samples (uvula) ($P = 0.0004$), after normalisation to RPLPO. (B–E) In situ hybridisation on hypopharyngeal tumour sections to localise **LOC92912** mRNA using sense (negative controls, B,C) and antisense (D,E) probes. Invasive epithelium (black arrow heads) and cancer tissue (yellow arrow heads) are indicated. Slides were counterstained with nuclear fast red (red/pink). (F–H) Immunohistochemistry detection of **LOC92912** protein using antibodies raised against **LOC92912** (peptide LPTGQNGTTEEVTSSE). (F) Pre-immune serum; (G,H) specific serum.

Homo sapiens (ref: NP_060052.1—NICE-5 protein): 91.55%/71 amino acids, *Caenorhabditis elegans* (ref: NP_492764.1—F25H2.8.p): 44.76%/361 amino acids], but not in bacteria, viruses, fungi or plants. LOC92912 is predicted to be a mainly nuclear soluble protein (56.5% nuclear, 17.4% mitochondrial, 17.4% cytoplasmic, 4.3% cytoskeletal, and 4.3% vesicular; EMBL Bioinformatic Harvester) and apparently does not contain a nuclear localisation signal [PredictNLS online (<http://cubic.bioc.columbia.edu/predictNLS/>)]. According to the SMART database, there are two structural domains, an N-terminal RWD domain (amino acids 8–23), and a C-terminal ubiquitin conjugating enzyme domain, UQ-CON (amino acids 207–368), connected by a coiled-coil (amino acids 133–163) (Fig. 1B). According to the NCBI Conserved Domain database, the C-terminal domain (amino acids 207–368) is highly conserved among species, suggesting that the protein has an important function.

Expression pattern of human LOC92912 in HNSCC

To characterise the expression of LOC92912, quantitative real time PCR (QRT-PCR) analysis was performed on RNA extracted from different HNSCC tumours. The transcript was found to be over-expressed in 12 out of 14 tumours (~85%), by an average of 2.4-fold compared to normal ($P = 0.0004$; Fig. 2A). To localise LOC92912, we performed both in situ hybridisation (ISH) and immunohistochemistry (IHC) analysis on tumour tissue sections from the same patients. Strong signals were observed in tumour cell islets, invasive epithelia, and dysplastic regions of the tumours, by both ISH and IHC (Figs. 2B–H). There were different levels of immunoreactivity in the 17 samples analysed: high in 6, moderate in 9, and none in 2. Similar results were observed by in situ hybridisation. The highest immunoreactivity was in the cytoplasm of epithelial cells.

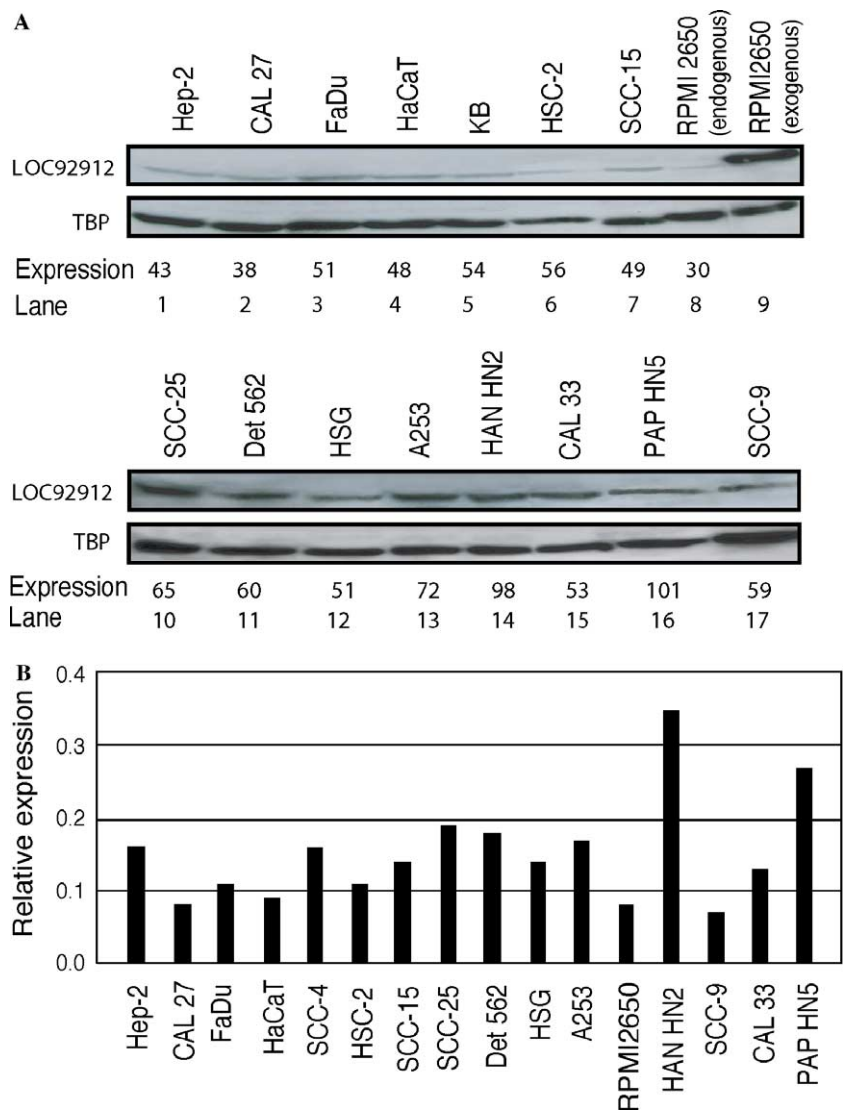


Fig. 3. LOC92912 expression in HNSCC cell lines. (A) Western blot analysis of cell extracts. The LOC92912 antibody recognises a ~43 kDa protein (lanes 1–8 and 10–16) and transfected flagged-LOC92912 (lane 9; ~45 kDa, 386 amino acids). Relative expression was calculated with respect to the TATA-binding protein (TBP; internal loading control). (B) QRT-PCR. Expression is normalised to RPLPO.

Expression of the human **LOC92912** in cell lines

We raised a rabbit polyclonal antibody (see Materials and methods) that specifically detected the transfected flagged-protein by Western blotting (Fig. 3A, lane 9, ~45 kDa). This antibody detected an endogenous polypeptide of the expected size (~43 kDa) in extracts from several HNSCC cell lines. The expression appeared to be relatively low when compared with the internal control (TBP). Similarly, QRT-PCR analysis (Fig. 3B) gave relatively weak signals, consistent with low expression at the RNA as well as the protein levels. The highest levels were found in PAP-HN5 and HAN-HN2.

Localisation of **LOC92912** in cell lines

The intracellular localisation of **LOC92912** was determined by immunofluorescent analysis of HEp-2 and HaCaT cells using both specific and anti-flag antibodies. The endogenous protein was mainly cytoplasmic (Fig. 4A). The transfected protein in RPMI cells was both cytoplasmic and nuclear (Fig. 4B), as confirmed by confocal microscopy (data not shown). Although the nuclear localisation may be a consequence of over-expression, it would agree with the bioinformatics analysis (see above).

Identification of **LOC92912** interacting proteins

We established a set of RPMI cells stably transfected with flagged-**LOC92912**. Potential interacting partners were identified by immunoaffinity chromatography of flagged-**LOC92912**, SDS-PAGE, and MALDI PMF mass spectrometry (Fig. 5). Fourteen silver-stained bands were excised, digested in the gel with trypsin and subjected to MALDI analysis. Nine bands gave specific spectra and 10 different human proteins were successfully identified. Among them, we found the **LOC92912** protein (lane 2, band d), actin and six actin-binding proteins (bands a, b, and e–h). Two of these proteins were also found in parallel control experiments using an unrelated flagged-protein (lane 2, bands c and e; lane 4, bands i and j; data not shown), suggesting that they are nonspecific interactors. No silver-stained bands were visible in the other control experiments using the empty (not shown), antisense **LOC92912** (lane 1) or control (lane 3) vectors. Altogether, these results indicate that actin and the six actin-binding proteins are **LOC92912** specific potential interactors, therefore suggesting that **LOC92912** has a function in cytoskeleton structure and/or regulation.

Discussion

In this study, we characterised a novel putative member of the E2 ubiquitin conjugating enzyme family, **LOC92912**, which is upregulated in HNSCC. We initially identified a sequence upregulated in hypopharyngeal tumours by differential display analysis [7] and then showed that it corre-

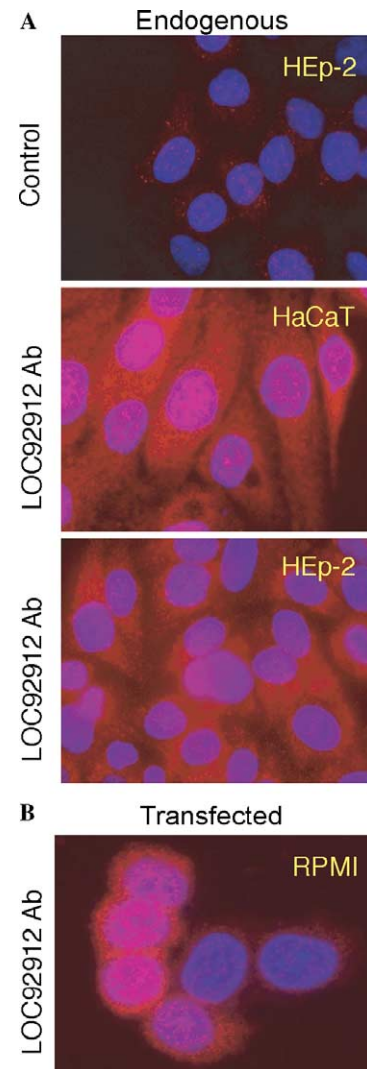


Fig. 4. Cellular localisation of **LOC92912** by indirect immunofluorescence. (A) Endogenous protein in Hep-2 and HaCaT cells. The control lacks primary antibody (Ab). (B) Transfected flagged-**LOC92912**. Nuclei were stained with DAPI and images were taken with 63× objective. Original magnifications: 400×.

sponds to the 3' end of a novel human gene, **LOC92912**. The striking conservation of **LOC92912** sequence homology among species, particularly in the predicted catalytic domain of the carboxy terminal half of the protein, suggests that it has an important catalytic function [10]. The amino terminal domain of **LOC92912** contains an RWD-domain related structure that has been found in about 100 proteins [10]. The domain is named after the three major RWD-containing proteins: RING finger-containing proteins, WD-repeat-containing proteins, and yeast DEAD (DEXD)-like helicases. It may be involved in protein–protein interactions and has been suggested to be a substrate recognition domain for ubiquitin-conjugating enzymes [10,11].

Multiple enzymes are involved in ubiquitination: the E1 enzyme activates ubiquitin and transfers it to a member of the E2 class of ubiquitin-conjugating enzymes; the E2

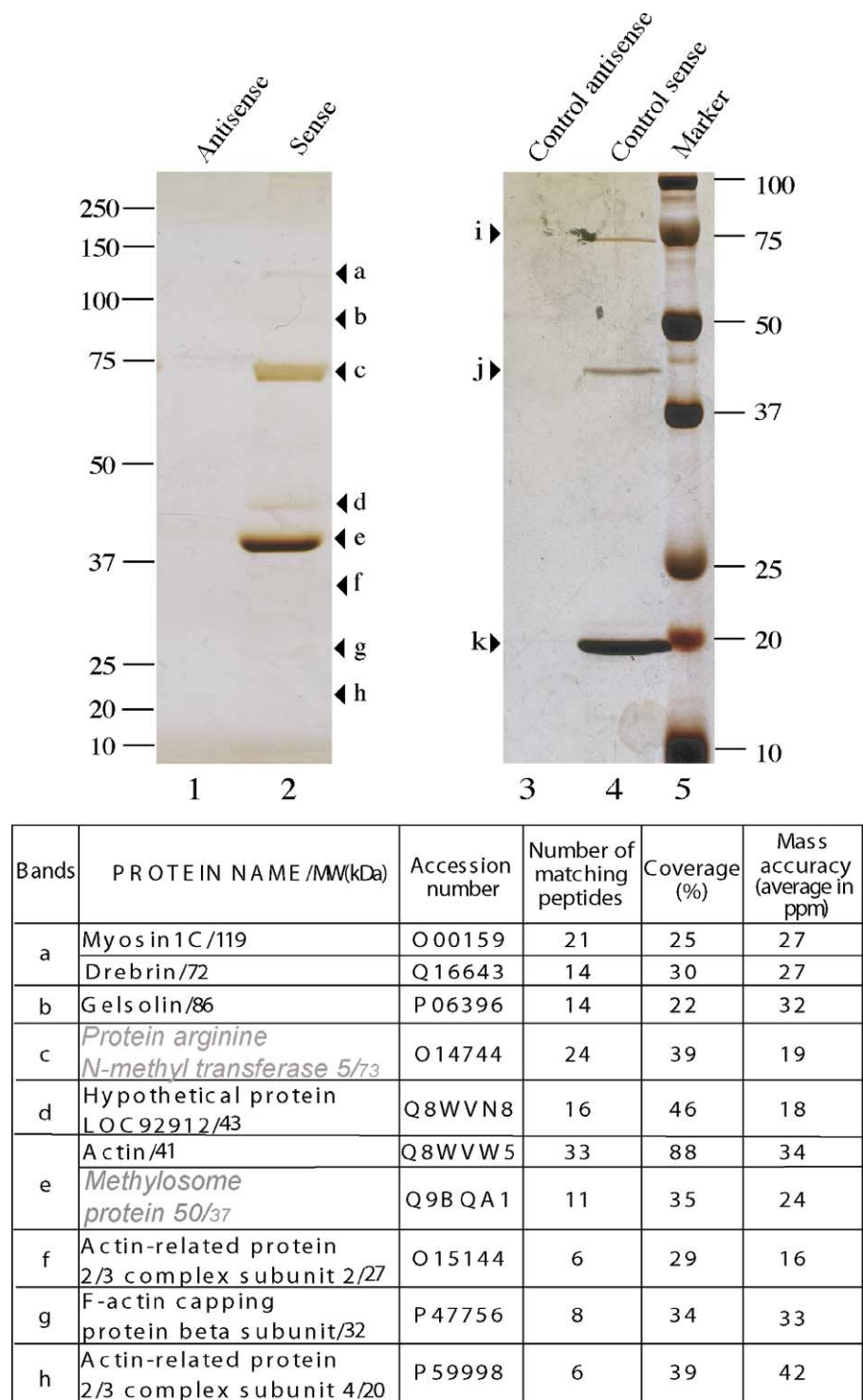


Fig. 5. Identification of proteins associated with **LOC92912** by immunoaffinity purification. Top panel: Representative silver-stained gels (lanes 1, 2, 8% gel; right, lanes 3–5, 12% gel) showing the band patterns of column eluates prepared from various stable clones. Lane 1, antisense-**LOC92912**; lane 2, sense-flagged-**LOC92912**; lane 3, unrelated control flagged-protein; lane 4, sense flagged control protein; lane 5, size marker. In the control sense (lane 4), the identification of i (protein arginine N-methyl transferase 5) and j (methylosome protein 50) was based on the following data; (i): number of matching peptides: 19, sequence coverage: 35%, Δm : 30 ppm; (j): number of matching peptides: 10, sequence coverage: 44%, Δm : 14 ppm; (k): number of matching peptides: 11, sequence coverage: 81%, Δm : 24 ppm; Δm : Delta mass/average mass accuracy. Bottom panel: identities of bands a–h determined by mass spectrometry. Note that c and i as well as e and j are the same proteins.

enzymes alone or in combination with E3 ubiquitin ligases transfer ubiquitin to these substrates. There are a relatively large number of different E2 and E3 enzymes that display specificity for groups of specific substrates [12]. Monoubiquitination and polyubiquitination have been shown to target proteins for degradation in the 26S proteasome [13], to target

proteins to the endocytic pathway, and also to functionally activate specific proteins [14]. Ubiquitination regulates critical signal transduction pathways, transcription factors [15,16], apoptosis proteins [17], cell cycle regulatory proteins [18], and tumour suppressors [19]. The potential role of **LOC92912** in ubiquitination and the utility of targeting this activity for tumour therapy [20] remains to be investigated.

LOC92912 mRNA was found to be overexpressed in 85% of tumours compared to the corresponding normal tissue. **LOC92912** mRNA and protein are localised in the invasive epithelium and cancer islets of hypopharyngeal tumour samples. The protein was also detected in several HNSCC cell lines, although the expression level was relatively low compared to an internal control. Highest levels of expression were observed in HAN-HN2 and POP-HN5 cells, and the lowest in SCC9 and CAL27 (tongue), RPMI2650 (nasal septum), and HaCaT cells (a nontumorigenic cell line derived from the periphery of a primary melanoma). The protein expression levels correlated with the mRNA levels obtained by QRT-PCR.

We showed that the endogenous protein is mostly localised to the cytoplasm, in cell lines as well as in tissues. Transfected over-expressed protein was also detected in the nucleus by confocal microscopy (data not shown). This could be an artefact of overexpression, although bioinformatics analysis also predicts nuclear localisation (EMBL Bioinformatics Harvester).

We found that actin and actin-associated proteins specifically copurify with **LOC92912**. Interestingly, the *Caenorhabditis elegans* homolog of **LOC92912** (NP_492764.1) is functionally involved in the cytoskeleton and movement of the organism [11]. Preliminary data using established stable cell lines indicate that over-expression of **LOC92912** alters cell shape and attachment to the substrate (data not shown). In conclusion, we present here a novel human gene that is upregulated in HNSCC cancers that could have actin related cytoskeletal functions. It will be interesting to investigate the roles of **LOC92912** in cell shape, migration, attachment to the substrate and survival, and to identify potential substrates for ubiquitination.

Acknowledgments

We thank Ingrid Colas for the mass spectrometry analysis, Annaïck Carles for help with the bioinformatics, Christine Macabre for excellent technical assistance, Jillian Howlin for critically reading the manuscript, members of the Wasylyk laboratory for friendship, support, and help, and the IGBMC core facilities. We acknowledge the Ministry of Health and Medical Education of IRAN and Shiraz University of Medical Sciences for a scholarship for A. Seghatoleslam. We thank for financial support: the Ligue Nationale Française contre le Cancer (Equipe Labellisée), the Ligues Départementales de Lutte contre le Cancer (Haut- and Bas-Rhin), the Centre National de la Recherche Scientifique, the Institut National de la Santé et de la Recherche Médicale, the Université Louis Pasteur,

the Association pour la Recherche sur le Cancer, and the European Union (FP5 Procure project QLK6-2000-00159 and FP6 Prima Project #504587).

References

- [1] G.M. Howell, J.R. Grandis, Molecular mediators of metastasis in head and neck squamous cell carcinoma, *Head Neck* 27 (2005) 710–717.
- [2] K.W. Forastiere, A. Trotti, D. Sidransky, Head and neck cancer, *N. Engl. J. Med.* 345 (2001) 1890–1900.
- [3] A. Jovanovic, E.A. Schulten, P.J. Kostense, G.B. Snow, I. van der Waal, Tobacco and alcohol related to the anatomical site of oral squamous cell carcinoma, *J. Oral. Pathol. Med.* 22 (1993) 459–462.
- [4] S.P. Schantz, T.C. Hsu, N. Ainslie, R.P. Moser, Young adults with head and neck cancer express increased susceptibility to mutagen-induced chromosome damage, *JAMA* 262 (1989) 3313–3315.
- [5] H.-H.M. Greenlee, T. Murray, M. Thun, Cancer statistics, 2001, *CA Cancer J. Clin.* 51 (2001) 15–36.
- [6] J. Akervall, Gene profiling in squamous cell carcinoma of the head and neck, *Cancer Metastasis Rev.* 24 (2005) 87–94.
- [7] F. Lemaire, R. Millon, J. Young, A. Cromer, C. Wasylyk, I. Schultz, D. Muller, P. Marchal, C. Zhao, D. Melle, L. Bracco, J. Abecassis, B. Wasylyk, Differential expression profiling of head and neck squamous cell carcinoma (HNSCC), *Br. J. Cancer* 89 (2003) 1940–1949.
- [8] A. Cromer, A. Carles, R. Millon, G. Ganguli, F. Chalmel, F. Lemaire, J. Young, D. Dembele, C. Thibault, D. Muller, O. Poch, J. Abecassis, B. Wasylyk, Identification of genes associated with tumorigenesis and metastatic potential of hypopharyngeal cancer by microarray analysis, *Oncogene* 23 (2004) 2484–2498.
- [9] N. Cavusoglu, M. Brand, L. Tora, A. Van Dorsselaer, Novel subunits of the TATA binding protein free TAFII-containing transcription complex identified by matrix-assisted laser desorption/ionization-time of flight mass spectrometry following one-dimensional gel electrophoresis, *Proteomics* 3 (2003) 217–223.
- [10] M.H. Melner, N.A. Ducharme, A.R. Brash, V.P. Winfrey, G.E. Olson, Differential expression of genes in the endometrium at implantation: upregulation of a novel member of the E2 class of ubiquitin-conjugating enzymes, *Biol. Reprod.* 70 (2004) 406–414.
- [11] E. Schulze, M.E. Altmann, I.M. Adham, B. Schulze, S. Frode, W. Engel, The maintenance of neuromuscular function requires UBC-25 in *Caenorhabditis elegans*, *Biochem. Biophys. Res. Commun.* 305 (2003) 691–699.
- [12] A.L. Haas, T.J. Siepmann, Pathways of ubiquitin conjugation, *FASEB J.* 11 (1997) 1257–1268.
- [13] S. Polo, S. Sigismund, M. Faretta, M. Guidi, M.R. Capua, G. Bossi, H. Chen, P. De Camilli, P.P. Di Fiore, A single motif responsible for ubiquitin recognition and monoubiquitination in endocytic proteins, *Nature* 416 (2002) 451–455.
- [14] K.D. Wilkinson, Ubiquitination and deubiquitination: targeting of proteins for degradation by the proteasome, *Semin. Cell Dev. Biol.* 11 (2000) 141–148.
- [15] J.M. Desterro, M.S. Rodriguez, R.T. Hay, Regulation of transcription factors by protein degradation, *Cell. Mol. Life Sci.* 57 (2000) 1207–1219.
- [16] M. Fan, X. Long, J.A. Bailey, C.A. Reed, E. Osborne, E.A. Gize, E.A. Kirk, R.M. Bigsby, K.P. Nephew, The activating enzyme of NEDD8 inhibits steroid receptor function, *Mol. Endocrinol.* 16 (2002) 315–330.
- [17] V. Jesenberger, S. Jentsch, Deadly encounter: ubiquitin meets apoptosis, *Nat. Rev. Mol. Cell Biol.* 3 (2002) 112–121.
- [18] A. Hershko, A. Ciechanover, The ubiquitin system, *Annu. Rev. Biochem.* 67 (1998) 425–479.
- [19] M. Li, D. Chen, A. Shiloh, J. Luo, A.Y. Nikolaev, J. Qin, W. Gu, Deubiquitination of p53 by HAUSP is an important pathway for p53 stabilization, *Nature* 416 (2002) 648–653.
- [20] N.H. Nam, K. Parang, Current targets for anticancer drug discovery, *Curr. Drug Targets* 4 (2003) 159–179.